AJNR

An in vivo arteriovenous malformation model in swine: preliminary feasibility and natural history study.

J C Chaloupka, F Viñuela, J Robert and G R Duckwiler

AJNR Am J Neuroradiol 1994, 15 (5) 945-950
http://www.ajnr.org/content/15/5/945

An In Vivo Arteriovenous Malformation Model in Swine: Preliminary Feasibility and Natural History Study

John C. Chaloupka, Fernando Viñuela, John Robert, and Gary R. Duckwiler

PURPOSE: To assess the feasibility, natural history, and preliminary physiologic validation of creating an in vivo arteriovenous malformation model in swine. **METHODS:** A transorbital puncture technique into the cavernous sinus was used to create an arteriovenous communication between the rostral rete and the cavernous sinus in eight swine. Short-term patency and hemodynamic behavior were assessed clinically and by serial angiography. Acute phase physiologic characterization of four models was also performed, using intravascular pressure and Doppler blood flow velocity measurements. **RESULTS:** Large arteriovenous shunts between the rostral rete and cavernous sinus were consistently produced, which mimicked the angiographic features of cerebral arteriovenous malformations in humans. Classic changes in intraarterial and intravenous pressures and blood flow velocities were also observed. Early pathophysiologic evolution occurred in two animals, consisting of recruitment of previously unseen collateral vessels. Spontaneous occlusion of the arteriovenous shunt occurred in most animals within 7 days because of a rigorous fibroblastic response. **CONCLUSIONS:** A simple technique for creating an arteriovenous malformation model in swine is now possible and is promising for future studies.

Index terms: Arteriovenous malformations; Animal studies; Interventional neuroradiology, models

AJNR Am J Neuroradiol 15:945–950, May 1994

For over a decade there has been keen interest in developing in vivo and in vitro arteriovenous malformation models by both neurosurgeons and interventional neuroradiologists. The former group has focused most of its attention on studying specific issues of cerebral arteriovenous malformation pathophysiology (steal, vasoreactivity, venous hypertension, etc) (1–5); the latter group has emphasized both testing and training issues related to endovascular embolotherapy (6–11). The previously described in vivo models have consisted of simple arteriovenous fistulas of the carotid circulation; the in vitro models have been crude plastic renderings of either arteriovenous fistulas or arteriovenous malformations. In both cases it is commonly acknowledged that there are significant limitations with these models.

Therefore, there remains a great need for a good in vivo arteriovenous malformation model, which can be used for both experimental pathophysiologic and therapeutic purposes. Theoretically, such an experimental model must possess two fundamental and essential components. The first is a structure that simulates the anatomic configuration of an arteriovenous malformation nidus; the second is an arteriovenous shunt related to the first component.

Certain ungulates of the order Artiodactyla (which includes swine) possess a rete mirabile. This structure is a plexiform network of interconnected microarteries in the size range of 50 to 250 μm enclosed by the cavernous sinuses at the skull base. The anatomic configuration of the rete strongly resembles the gross and angiographic morphology of an arteriovenous malformation nidus (Fig 1).

Consequently, the swine rete has been used as a model of an arteriovenous malformation nidus for testing the efficacy and histotoxicity of embolic agents and techniques (10–12). The major limitation of this model, however, is that the rete

Received February 5, 1993; accepted for publication May 28.

From the Endovascular Therapy Service (J.C.C., F.V., G.R.D.) and the Leo Rigler Laboratory (J.R.), Department of Radiological Sciences, UCLA Medical Center, Los Angeles, CA 90024.

Address reprint requests to John C. Chaloupka, MD, Interventional Neuroradiology, Department of Radiology, Yale University School of Medicine, 333 Cedar St, PO Box 3333, New Haven, CT 06510.

AJNR 15:945–950, May 1994 0195-6108/94/1505–0945

consists of low-flow, high-resistance arterio-arterial connections, in which the major inflow vessel is the ascending pharyngeal artery, and the major outflow vessel is the internal carotid artery (Fig 1). Thus, the rete system in its natural state lacks the important second requirement for a good in vivo arteriovenous malformation model, a shunting arteriovenous communication.

After performing numerous dissections and detailed anatomic studies of the swine rete and cavernous sinus, we realized that this second requirement for creating an in vivo arteriovenous malformation model was theoretically possible. Because the rete is completely surrounded by a low-pressure venous system (the cavernous sinus) and has only one major outflow vessel (the internal carotid artery), a high-flow arteriovenous shunt could possibly be produced by surgically diverting the arterial outflow from the origin of the internal carotid artery into the cavernous sinus.

The objectives of this preliminary study were to assess the feasibility and efficacy of creating a true in vivo arteriovenous malformation model in swine and to study the natural history and clinical behavior of this model. Our initial experience in physiologic characterization of the short term hemodynamic behavior of this model is also presented.

Materials and Methods

The experiments were performed in accordance with guidelines for the use of laboratory animal subjects in research by the University of California-Los Angeles Chancellor's Animal Research Committee and the National Institutes of Health. Eight Red Duroc swine were first sedated with intramuscular diazepam (0.5 mg/kg) and ketamine (20 mg/kg). After intubation, general anesthesia was induced and maintained with continuous inhalation of 1% to 1.5% halothane.

Creation of an arteriovenous shunt between the outflow of the rostral rete (including the internal carotid artery) and the cavernous sinus was accomplished through a novel transorbital puncture technique. An 18-gauge spinal needle was inserted anteroinferiorly through the orbit by an intraconal-retrobulbar pathway. The needle was then directed medially and caudally through the foramen orbitorotundum, through which the anterior and rostral cavernous sinus was then entered (Fig 2).

Using a combination of fluoroscopic guidance, cavernous sinography, and digital road mapping, we created an arteriovenous communication strategically located between the rostral rete and the cavernous sinus by manipulating the bevel of the needle as if performing a percutaneous biopsy. Particular effort was made to sever or puncture the origin of the internal carotid artery, which is intracavernous in location. Successful creation of the arteriovenous fistula was indicated by return of bright red blood through the cannula of the spinal needle.

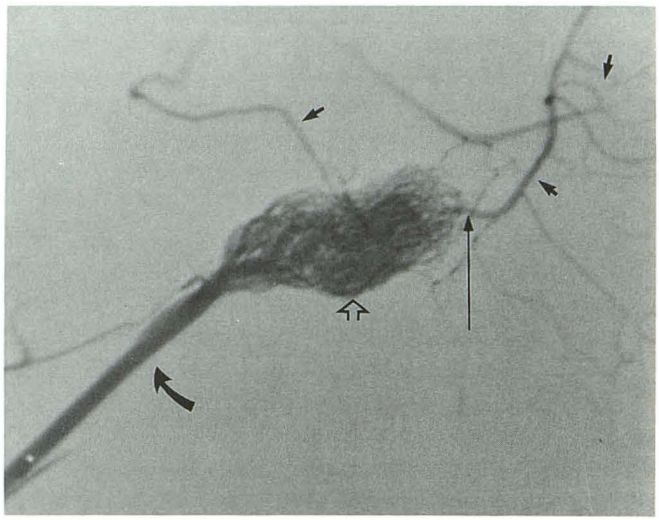

Fig. 1. Lateral angiogram of the swine carotid retial system, showing the ascending pharyngeal artery (*curved arrow*), rete mirabile (*open arrow*), internal carotid artery (*long arrow*), and major cerebral arteries (*small arrows*).

The hemodynamic behavior and natural history of each animal were assessed by clinical exam and serial angiography. The swine were examined daily for signs of hypertensive orbital venopathy, orbital bruit, orbital pain, and cerebral ischemia. Daily doses of bupernorphine (0.01 mg/kg, subcutaneously) were administered prophylactically to minimize orbital pain.

Angiography was usually performed at intervals of 3 to 5 days for up to 2 weeks to evaluate the short-term behavior of the model. Selective catheterization of both common carotid arteries and ipsilateral internal maxillary arteries was performed in all models with a modified tapering 5.5–4.0 French catheter (Cook, Bloomington, IN). Superselective catheterization of the ascending pharyngeal artery and occasionally the middle meningeal artery was also performed with a Tracker 18/Seeker 14 combination (Target Therapeutics, Fremont, Calif).

Physiologic characterization studies of these arteriovenous malformation models in the acute phase (ie, upon the day of creation of the model) were also performed. These validation studies consisted of two components. First, standard intravascular pressure measurements (13) were performed using a TNF-R fluid pressure transducer (Spectromed, Oxnard, Calif) and electronic analog amplifier/recorder (Hewlett-Packard, Waltham, Mass). Continuous monitoring of intraarterial pressures was accomplished by superselective catheterization of the ascending pharyngeal artery with a Tracker 18 microcatheter, or continuous monitoring of intravenous pressures was performed by cannulation of the cavernous sinus with the outer cannula

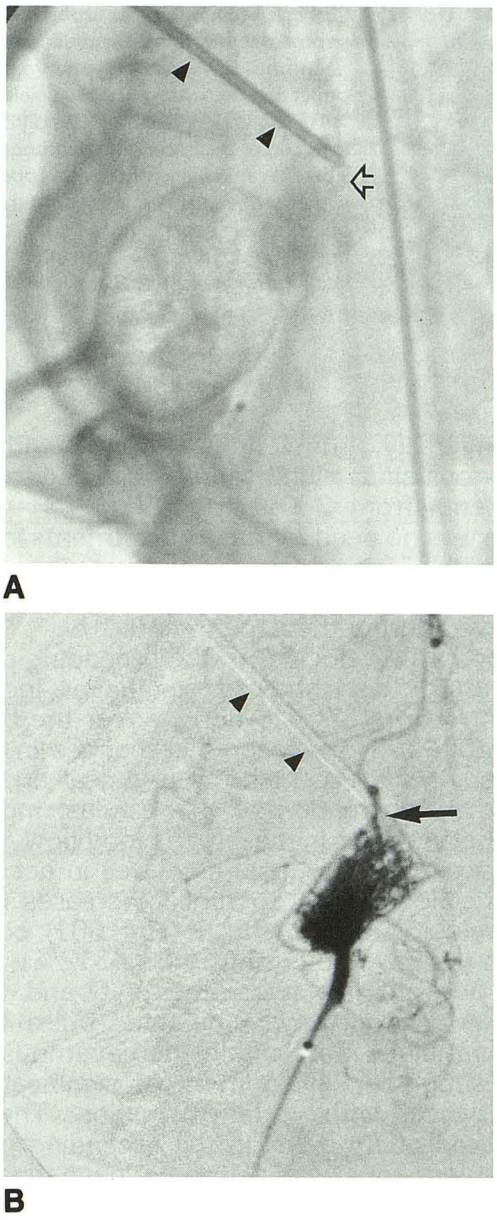

Fig. 2. Transorbital puncture technique for creation of the arteriovenous malformation model

A, Unsubtracted and *B*, subtracted ascending pharyngeal artery projection angiograms of the right retial system, showing the transorbital course of the spinal needle (*arrowheads*) into the rostral cavernous sinus (*open arrow*). Note the position of the tip of needle relative to the origin of the internal carotid artery (*arrow*).

of the 18-gauge spinal needle used for creating the arteriovenous fistula.

The second component of the physiologic characterization of the arteriovenous malformation model consisted of measurements of various intravascular blood flow velocity parameters with either a 0.018″ or 0.014″ Doppler microguidewire and spectrum analyzer (Flowire or Smartwire and FloMap, Cardiometrics, Mountain View, Calif). The Doppler spectra from the Doppler microguidewire provided continuous quantitative measurements of time-averaged peak velocity, maximum peak velocity, and computed pulsatility index [(maximum peak velocity − time-averaged peak velocity)/maximum peak velocity]. Our laboratory recently conducted in vivo validation studies for potential neuroendovascular applications of the 0.018-in Doppler microguidewire which showed that time-averaged peak velocity obtained by the Doppler microguidewire maintained a linear relationship with measured volumetric blood flow within a given vessel over a wide range of physiologic and superphysiologic blood flow conditions (14). The Doppler microguidewire was placed through either a Tracker 18 or 3 French catheter and positioned 1 cm below the rete for intraarterial measurements. Intravenous blood flow velocity measurements were taken by placing the Doppler microguidewire through the outer cannula of the spinal needle and positioning it in the rostral cavernous sinus.

Statistical analysis of the physiologic data was accomplished using a one-tailed paired *t* test. Values of *P* were calculated using Statview software (Brainpower, Calabasas, Calif), in which results were considered significant at $P < .05$.

Results

Large arteriovenous shunts between the rete and cavernous sinus were consistently produced and strongly resembled the angiographic characteristics of arteriovenous malformations (Figs 3 and 4). Superselective injections into the ascending pharyngeal artery showed rapid sequential filling of the rete, cavernous sinus(es), and basilar dural sinus(es). This series of observed structures closely simulated the sequential angiographic appearance of nidus, proximal varix, and cortical or dural venous drainage that is seen frequently in cerebral arteriovenous malformations in humans.

During the time that the arteriovenous shunt remained patent, proptosis, chemosis, and subconjunctival hemorrhage were consistently observed in the ipsilateral eye. In many cases an orbital bruit was also auscultated and was used as a means of assessing the patency of the shunt. No cranial nerve palsies or clinically detectable cerebral ischemia developed in any of the swine.

Spontaneous occlusion of the arteriovenous communications usually occurred within 5 to 7 days, although two fistulas lasted for at least 14 days. Gross and histologic analysis of the arteriovenous malformations that had spontaneously occluded showed intense inflammatory and fibroblastic responses in the rostral rete at the sites of incision by the spinal needle.

Acute phase physiologic characterization of the last four arteriovenous malformations was consistent with the most salient physiologic characteristics of cerebral arteriovenous malformations humans (Tables). Unadjusted measurements of intraarterial pressure in the ascending pharyngeal

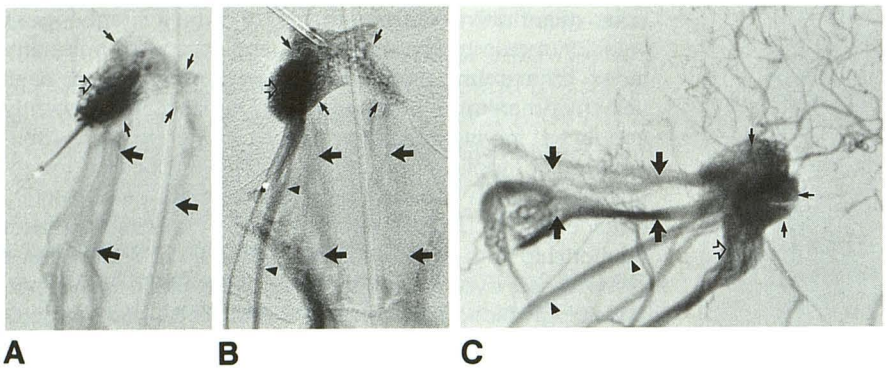

Fig. 3. Examples of three different experimental arteriovenous malformations.

A and *B*, Ascending pharyngeal artery projection.

C, Lateral projection angiograms from injection of the ascending pharyngeal artery. There is rapid filling of the rete (*open arrow*), with arteriovenous shunting into the cavernous sinuses (*short arrows*), basilar dural sinuses (*large arrows*), and internal jugular veins (*arrowheads*) in *B* and *C*.

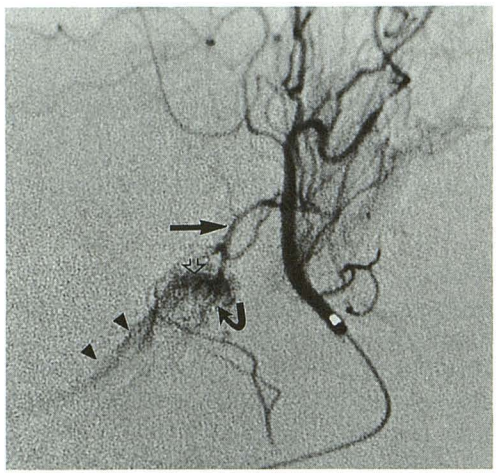

Fig. 4. Example of early collateral recruitment. Lateral projection angiogram from superselective injection of the middle meningeal artery, showing filling of the ramus anastomonicus (*long arrow*) and rostral rete (*curved arrow*). There is arteriovenous shunting into the cavernous sinus (*open arrow*) and basilar dural sinus (*arrowheads*).

artery consistently decreased from baseline in the range of 5% to 72% ($P = .02$). Because of the observed 4% to 7% decrease in systemic blood pressure that occurred in all experiments, relative changes in intraarterial pressure were adjusted as follows. Differences between mean systemic arterial pressure and mean arterial pressure within the ascending pharyngeal artery (ie, mean feeder arterial pressure) were calculated before and after creation of each model. This calculation of a perfusion gradient adjusted for any changes that may have occurred in systemic arterial pressure during the experiment. If a larger perfusion gradient (ie, difference between systemic arterial pressure and feeder pressure) was measured during a given experiment, then a "true" decrease in feeder arterial pressure occurred. In all experiments, the perfusion gradient increased from 11% to 86%, which was found to be statistically significant ($P = .043$).

Conversely, intravenous pressure within the cavernous sinus significantly increased in all experiments from 300% to 4000% ($P = .027$). There was no need to make adjustments in measurements of intracavernous venous pressure, because no changes in central venous pressure were observed during the experiments.

Blood flow velocities in the ascending pharyngeal artery also showed significant increases, ranging from 135% to 686%, over the baseline ($P = .0041$). No measurable changes in the diameter of the ascending pharyngeal artery occurred after creation of the fistulas, indicating that the increases in measured blood flow velocity represented proportional increases in actual volumetric blood flow (18). Similar increases in blood flow velocity, also significant ($P = .001$), occurred within the cavernous sinus (58%–312%).

In two animals (experiments 6 and 8), the Doppler microguidewire detected pulsatile bidirectional blood flow within the cavernous sinus, suggesting the development of significant flow disturbances with vortex formation. The computed pulsatility index in the ascending pharyngeal artery also was found to have decreased significantly in all animals (36%–63% decrease, $P < .027$), which indicated a decrease in downstream vascular resistance after creation of the arteriovenous malformation model.

In two different animals, there was evidence of what can be referred to as pathophysiologic evolution, in which within a period of 5 to 7 days, there was recruitment of one of the anastomotic vessels (ramus anastomonicus) supplying the rete seen on serial angiography. The ramus anastomonicus and arteria anastomonica in swine normally are very small and exist mostly as potential sources of collateral blood flow to the rete (15). These vessels are usually not seen on routine angiography of the external carotid system in healthy swine. In both models with pathophysiologic evolution, the ramus anastomonicus had not been seen at the time of the initial creation of the arteriovenous malformation

Intravascular pressure and blood flow velocity measurements before (baseline) and after creation of the arteriovenous malformation (AVM) model.

Acute physiologic studies: experiment 5

	Baseline	AVM Model	Change (%)
SAP	89	85	−4
HR	70	80	+14
Right AP			
APV	16	41	+156
CPI	1.05	0.39	−63
FAP	81	72	−11
SAP-FAP	7	13	+86
Right CS			
APV	12	19	+58
MVP	1	4	+300

Acute physiologic studies: experiment 6

	Baseline	AVM Model	Change (%)
SAP	92	85	−7.6
HR	87	90	+3.4
Right AP			
APV	12	36	+200
CPI	0.76	0.47	−36
FAP	29	8	−72
SAP-FAP	63	77	+22
Right CS			
APV	5.7	14; −18[a]	+146; +216
MVP	1	15	+1400

Acute physiologic studies: experiment 7

	Baseline	AVM Model	Change (%)
SAP	95	91	−4.2
HR	90	70	−22
Right AP			
APV	5.6	44	+686
CPI	0.58	0.38	−34
FAP	85	75	−12
SAP-FAP	10	16	+60
Right CS			
APV	3.4	14	+312
MVP	0	21	+2000

Acute physiologic studies: experiment 8

	Baseline	AVM Model	Change (%)
SAP	125	120	−4
HR	90	110	+22
Right AP			
APV	34	80	+135
CPI	0.5	0.3	−40
FAP	116	110	−5
SAP-FAP	9	10	+11
Right CS			
APV	8.1	18; −22[a]	+122; +172
MVP	2	11	+450

Note.—APV indicates average peak velocity; SAP, mean systemic arterial pressure; FAP, mean feeder arterial pressure; SAP-FAP, perfusion pressure gradient; MVP, mean venous pressure (all in mm Hg); HR, heart rate (in beats per minute); CPI, computed pulsitility index; AP, ascending pharyngeal artery; and CS, cavernous sinus.

[a] Negative Doppler velocity values indicate detection of blood flow toward the transducer.

model, suggesting that the hemodynamic balance of blood supply to the rete was altered over time by the arteriovenous shunt.

Discussion

We have described a relatively simple and reliable technique for creating a short-term arteriovenous malformation model in swine. This model simulates the basic anatomic and hemodynamic aspects of cerebral arteriovenous malformations. This experimental model is promising for a variety of applications, including pathophysiologic studies, embolotherapy research, and endovascular therapeutic training.

The acute phase, physiologic characterization studies of this in vivo arteriovenous malformation model show that it possesses the same fundamental features of cerebral arteriovenous malformations in humans. Intraarterial feeder pressure decreased, intravenous outflow pressure increased, and blood flow velocities increased in both the arterial feeder and venous outflow of the two studied models. Furthermore, the computed pulsatility index within the ascending pharyngeal artery significantly decreased, which provided semiquantitative confirmation of a decrease in downstream vascular resistance. All of these findings have been demonstrated in cerebral arteriovenous malformations in humans (13,16,17).

More comprehensive validation studies will be needed to characterize better the physiology of these models to determine their comparability with naturally occurring arteriovenous malformations. Future studies will require more intensive monitoring of additional physiologic parameters, such as P_{CO_2} and cardiac output, to provide a means of standardization of the observed hemodynamic changes in the arteriovenous malformation model.

The early recruitment of collateral vessels in some of the animals was a surprising and fascinating finding of this study. This observation provides further preliminary evidence of the comparable behavior of the experimental model to natural arteriovenous malformations. This pattern of pathophysiologic evolution is analogous to the well known phenomenon of arterio-arterial collateralization observed in some large cerebral arteriovenous malformations in humans.

There are some limitations with the current model for physiologic investigation. Although the nidus and arteriovenous shunt of the model are located in close proximity to the brain and are related to the intracranial circulation, the arteriovenous malformation is not intimately involved with the brain. This may pose some problems in studying the complex hemodynamic relationships between an arteriovenous malformation and

the surrounding cerebral microcirculation, because it is probable that at least some of the pathophysiologic consequences of cerebral arteriovenous malformations (eg, steal and venous hypertension) are caused by local phenomena occurring at the borders of an arteriovenous malformation nidus (17,18). Another potential problem with this model is that it is currently unknown whether it behaves as a unicompartmental or multicompartmental nidus. The observation of early recruitment of collateral supply to the simulated nidus suggests that the model may be functionally multicompartmental, although further investigation will be necessary to prove this. Finally, the current arteriovenous malformation model has the disadvantage of tending to occlude spontaneously because of a rigorous fibroblastic response. Without attempting to alter this process, the model is good only for short-term investigations.

From an endovascular therapeutic perspective, there are several immediate benefits of this in vivo arteriovenous malformation model. The model provides an improved means of testing the efficacy and safety of a variety of embolic materials and techniques, because it closely simulates both the microvascular anatomy and high-flow conditions of cerebral arteriovenous malformations in humans. Furthermore, because it is an in vivo model, it has the benefit of enabling evaluation of the effects of embolic agents on living tissue, such as acute endothelial toxicity, thrombogenesis, chronic histotoxicity, and histopathology. This feature of the model is necessary for studying embolic agents that have primarily a toxic effect on vascular endothelium (eg, sodium tetradecyl sulfate, Ethibloc, and alcohol).

The model's ability to simulate both the pathophysiologic and the anatomic characteristics of an arteriovenous malformation in combination with the swine being readily amendable to standard percutaneous catheterization techniques make it an excellent means for training of various established neuroendovascular techniques. This model is superior to the earlier in vitro embolization models (6–9), because it not only more closely simulates the anatomy and physiology of an arteriovenous malformation, but also allows actual practice of the same technical aspects of catheterization and endovascular embolization in humans. Furthermore, this model is more versatile, because it is suitable for demonstrating responses to both the physical occlusive behavior (eg, particulates and liquid adhesives) and vascular toxic effects (eg, sclerosants) of various embolic materials.

References

1. Scott BB, McGillicuddy JE, Seeger JF, Kindt GW, Giannotta SL. Vascular dynamics of an experimental cerebral arteriovenous shunt in the primate. *Surg Neurol* 1978;10:34–38
2. Spetzler RF, Wilson CB, Weinstein P, et al. Normal perfusion pressure breakthrough theory. *Clin Neurosurg* 1978;25:651–672
3. Morgan MK, Anderson RE, Sundt TM. The effects of hyperventilation on cerebral blood flow in the rat with an opened and closed carotid-jugular fistula. *Neurosurgery* 1989;24:606–611
4. Morgan MK, Anderson RE, Sundt TM. A model of the pathophysiology of cerebral arteriovenous malformations by a carotid-jugular fistula in the rat. *Brain Res* 1989;496:241–250
5. Bederson JB, Wiestler OD, Brustle O, Roth P, Frick R. Yasargil MG. Intracranial venous hypertension and the effects of venous outflow obstruction in a rat model of arteriovenous fistula. *Neurosurgery* 1991;29:341–350
6. Kerber CW, Bank WO, Cromwell LD. Calibrated leak balloon microcatheter: a device for arterial exploration and occlusive therapy. *AJR Am J Roentgenol* 1979;132:207–212
7. Kerber CW, Flaherty LW. A teaching and research simulator for therapeutic embolization. *AJNR Am J Neuroradiol* 1980;1:167–169
8. Debrun GM, Vinuela FV, Fox AJ, Kan S. Two different calibrated-leak balloons: experimental work and applications. *AJNR Am J Neuroradiol* 1982;3:407–414
9. artynski WS, O'Reilly GV, Forrest MD. High flow rate arteriovenous malformation model for simulated therapeutic embolization. *Radiology* 1988;167:419–421
10. Brothers MF, Kaufmen JCE, Fox AJ, Deveikis JP. *N*-Butyl 2- cyanoacrylate-substitute for IBCA in interventional neuroradiology; histopathologic and polymerization time studies. *AJNR Am J Neuroradiol* 1989;10:777–786
11. Lylyk P, Vinuela F, Vinters HV, Dion J, et al. Use of a new mixture for embolization of intracranial vascular malformations: preliminary experimental experience. *Neuroradiology* 1990;32:304–310
12. Chaloupka JC, Vinuela F, Cheng J, Watson V, Duckwiler GR. Technical feasibility and histopathologic studies of ethylene vinyl alcohol copolymer (EVAL) in the swine endovascular embolization model (abstr). *AJR Am J Roentgenol* 1993;160:1:15–116
13. Duckwiler G, Dion J, Vinuela F, Jabour B, et al. Intravascular microcatheter pressure monitoring: experimental results and early clinical evaluation. *AJNR Am J Neuroradiol* 1989;11:169–175
14. Chaloupka JC, Vinuela F, Kimme-Smith C, Robert J, Duckwiler G. Use of a Doppler microguidewire for intravascular blood flow measurements: a validation study for potential neuro-endovascular applications. *Am J Neuroradiol* (in press)
15. Daniel PM, Dawes JDK, Prichard MM. Studies of the carotid rete and its associated arteries. *Philos Trans R Soc Lond [Biol]* 1953;237: 173–208
16. Lindegaard KF, Grolimund P, Aaslid R, Nornes H. Evaluation of cerebral AVMs using transcranial Doppler ultrasound. *J Neurosurg* 1986;65:335–344
17. Rosenblum BR, Bonner RF, Oldfield EH. Intraoperative measurement of cortical blood flow adjacent to cerebral AVM using laser Doppler velocitometry. *J Neurosurg* 1987;66:396–399
18. Batjer HH, Devous MD, Meyer YJ, Purdy PD, Samson DS. Cerebrovascular hemodynamics in arteriovenous malformation complicated by normal perfusion pressure breakthrough. *Neurosurgery* 1988;22: 503–508